The Nature of Probability Density Functions in Turbulent Channel Flow

S. Raghuram

Abstract The nature of probability density functions of streamwise velocity, wall-normal velocity and Reynolds shear stress fluctuations is analysed for a turbulent channel flow using hotwire anemometry and particle image velocimetry measurements. The hotwire measurements are validated with data from literature. The particle image velocimetry measurements capture the probability density functions well albeit at a smaller acquisition sampling rate when compared to hotwire. The probability density functions of the streamwise and the wall-normal velocity fluctuations exhibit Gaussian behaviour close to the wall at least till the end of the inertial sublayer, while the probability density functions of Reynolds stress fluctuations exhibit non-Gaussian, peaky behaviour throughout the channel, depicting the episodic nature of turbulence production.

Keywords Turbulent channel flow · Probability density function · Gaussian distribution · Log region

1 Introduction

Probability density function (PDF) of fluctuating quantities is an important statistical property of turbulence. Quantities computed from PDFs have the same value if the PDF profiles are identical. A new definition for the logarithmic region was defined by ref. [1] to be the wall-normal extent, in which the PDF profiles of streamwise velocity fluctuations are invariant, using hotwire (HW) measurements in a low Reynolds number zero pressure gradient (ZPG) turbulent boundary layer (TBL). They also find the PDF profiles of streamwise velocity fluctuations to be close to Gaussian distribution in the logarithmic region. This invariance is later tested for higher Reynolds numbers using KTH database for ZPGTBL by ref. [2]. It is found that the region of self-similarity extends from 160 wall units to 0.3 BL thicknesses. This region is

S. Raghuram (✉)
Department of Aerospace Engineering, Indian Institute of Science Bangalore, Bengaluru 560012, India
e-mail: ssrinivasan@iisc.ac.in

K. M. Singh et al. (eds.), *Fluid Mechanics and Fluid Power, Volume 2*, Lecture Notes in Mechanical Engineering, https://doi.org/10.1007/978-981-99-5752-1_5

larger than and includes the universal overlap region. While the self-similarity of the PDF of streamwise fluctuations has been studied in detail, not much has been reported on the nature of PDF of the wall-normal and shear stress fluctuations.

From detailed experiments in a neutrally stable atmospheric boundary layer, [3] distinguished between productive and counter-productive momentum flux events and periods in the time domain. They contended that these productive/counter-productive events and idle events (that produce no momentum flux) are, respectively, similar to the concept of active and inactive motions introduced by Townsend. They noted that low-flux fluctuations (typically less than a standard deviation in the flux) make little net contribution to the mean flux, and so could perhaps be termed passive motion. The more intense fluctuations are 'active' in the generation of flux. It was suggested therein that the passive motion is best described in the language of waves and harmonic analysis, whereas the active motions (productive or counter-productive)—could usefully be viewed as a series of events, possibly related to certain strongly coherent motions.

Episodic nature of the signals can be analysed using PDFs. The signals can be characterized to be episodic if the PDF exhibits a peaky behaviour. In particular, if the most probable value or the mean value is zero and centred at the peak and nonzero values are lot less frequent. An example of a similar distribution for $u'v'$ was noticed by ref. [4] and such a peaky non-Gaussian distribution was deemed therein to be transitional. In this paper, the Gaussian nature of the streamwise velocity fluctuations in the logarithmic region is confirmed using particle image velocimetry (PIV) data for a turbulent channel flow. Further, the nature of PDFs of wall-normal and Reynolds shear stress fluctuations is analysed, their Gaussian-ness in the log region explored. The paper is organized into four sections. The Sect. 2 deals with details of the measurements made, Sect. 3 discusses the main results in the paper and the final Sect. 4 summarizes the findings of the study.

2 Experimental Details

Data from measurements conducted in a TCF using HW (at $Re_\tau = 1537$) and PIV (at $Re_\tau = 1400,1559$) are used in the present study. The inflow to the channel is through a wind tunnel section and connects to the channel through a contraction with high area contraction ratio (CR) as shown in Fig. 1. The effective CR of the contractions C1 (CR of 8.3) and C2 (CR of 13) connected in series is 108, thereby making the flow in the tunnel very quiet. The details of the tunnel design and the measurement techniques used can be found from [5].

Two-dimensional instantaneous velocity field is measured (in the streamwise wall-normal plane) using a LaVision FlowMaster PIV system, consisting of a double-pulsed Nd:YAG laser (Litron Lasers—Nano L PIV Series) with repetition rate of 15 Hz. A CCD camera (Imager SX) with 4 megapixel resolution fitted with a Nikon macro lens having a focal length of 105 mm (AF-S VR MICRO-NIKKOR 105MM F/2.8G IF-ED) is used to capture the images of the seeded particles, introduced at the

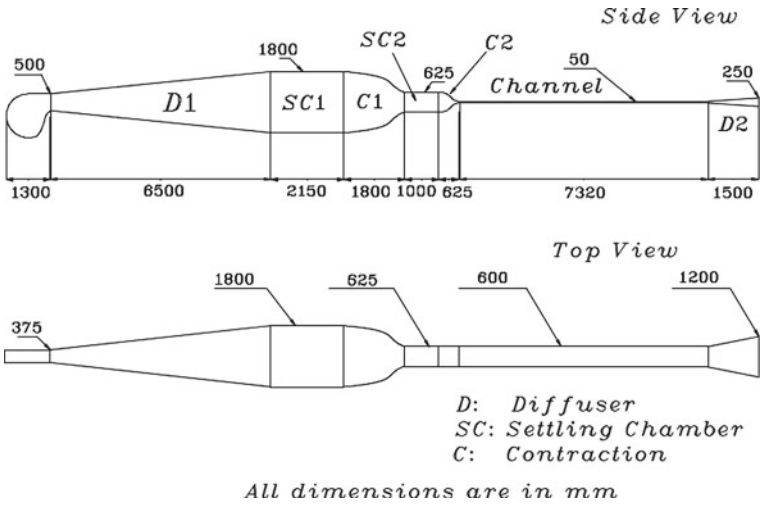

Fig. 1 Channel tunnel design drawing

blower inlet. The experiments were carried out and post-processed using the Davis 8.4.0 commercial software. The PIV measurements (at $Re_\tau = 1400, 1559$) used in the present study have been acquired and processed for 5 min (4500 images).

Hot wire anemometer is used to measure streamwise velocity fluctuations using a probe built in-house. The probe consists of two steel prongs (10 mm long, spaced at 0.8 mm from each other), where the sensor element is soft-soldered onto its tips. The sensor element is a Wollaston wire (manufactured by Sigmund Cohn Corp., USA) with a Pt–Rh core wire of diameter 5 microns protected by a silver outer coating. The active length of the sensor is kept typically around 0.5 mm. The viscous-scaled wire length $l^+ = lu_\tau/\nu \approx 30$ in this study for the highest speed case and $l/d \approx 100$. The prongs are inclined at an angle of 45° with the axis of the tube, so that the measurement is free from disturbance due to a part of the probe being in the downstream of the sensor, especially in the same wall-normal plane. The hot wire is operated by DANTEC DYNAMICS miniCTA (constant temperature anemometer) unit with a sampling frequency of 10 kHz. The unit was operated with a constant overheating ratio of 1.5. A National Instruments M Series NI PCI-6251 A/D card (16-bit resolution) was used for converting the analogue signals to digital voltage data. The HW is connected to a Mitutoyo height gauge, which is used as a traverse in the wall-normal direction and has a least count of 0.01 mm.

The probe is calibrated in situ to avoid drifts associated with moving the probe between tunnels and re-inserting. This is done by taking measurements at various y-locations and comparing them with measurements from Pitot tube at the same locations. Hence, separate measurements are not performed exclusively for the calibration. The probe is then calibrated using the standard King's law $V^2 = A + BU^n$, $n = 0.5$. The near-wall measurements using HW are disturbed by the conduction or convection heat loss to the wall, leading to velocities higher than the actual value.

This is corrected by employing a heat transfer correction to the acquired signal given by ref. [6]. The HW measurements (at $Re_\tau = 1537$) used in the present study has been acquired and processed for 1 min (600,000 data points). The velocity obtained from HW measurements is plotted in semilog scale in Fig. 2a for $Re_\tau = 1537$ along with Pitot measurements at the same speed. The curves follow the standard log-law shown by dashed lines in the inertial sublayer (ISL) with a slope, $\kappa = 0.37$. The quality of the velocity data in the near-wall region is excellent, follows $u^+ = y^+$variation faithfully in the viscous sublayer (linear region) as expected. HW data from [7] is also plotted at $Re_\tau = 1543$ and has nearly the same slope, with slightly lower intercept. Streamwise intensity is next plotted in Fig. 2b along with HW data of [7] at $Re_\tau = 1543$ and that of [8] at $Re_\tau = 1524$ and the agreement with the present data is good. The peak of present data matches with that of [7], while the peak of [8] is slightly higher.

The PDF of fluctuating streamwise velocity for $Re_\tau = 1559$ using present PIV data (denoted by dashed lines) is plotted with corresponding HW data for $Re_\tau = 1537$ (denoted by solid lines) at various heights from the wall in Fig. 3. It can be seen that the PDF of u from PIV measured with sampling rate of 15 Hz compares well at various heights throughout the channel with u PDF of HW at similar heights measured with sampling rate of 10 kHz. This shows that the PDF of u is captured well by PIV measurements despite its lower sampling rate.

3 Results and Discussion

The PDFs of streamwise and wall-normal velocity fluctuations are, respectively, shown in Figs. 4 and 5 for $Re_\tau = 1400$ using the PIV data. While the solid lines denote the PDF of the fluctuations, the dashed lines denote the corresponding Gaussian curves with the same mean and standard deviation as the fluctuations at a given wall-normal location. The PDF of streamwise velocity fluctuations looks closely Gaussian, especially at small values of y^+ and there is departure from that trend as one moves to the outer region as shown in Fig. 4. The PDFs of streamwise velocity are also positively skewed and the skewness decreases with y^+. In Fig. 5, again the wall-normal velocity looks closely Gaussian at small values of y^+ but looks more negatively skewed as one moves outward towards the core region. The wall-normal velocity fluctuations exhibit less skewness than the streamwise velocity fluctuations.

The PDF of the Reynolds stress is shown for the same Reynolds number in Fig. 6. The profiles look less Gaussian and a more peaky kind of distribution is observed centred around a zero mean value, though u' and v' are themselves Gaussian. It is interesting to note the observation of [4] who got such peaky PDFs of Reynolds stress with zero mean and was seen to correspond to intermittent behaviour. In other words for most of the duration, the Reynolds stress is hovering around a zero value and every once in a while due to a strong event a large value of $-u'v'$ may be produced. This would be called a productive or episodic event according to [3].

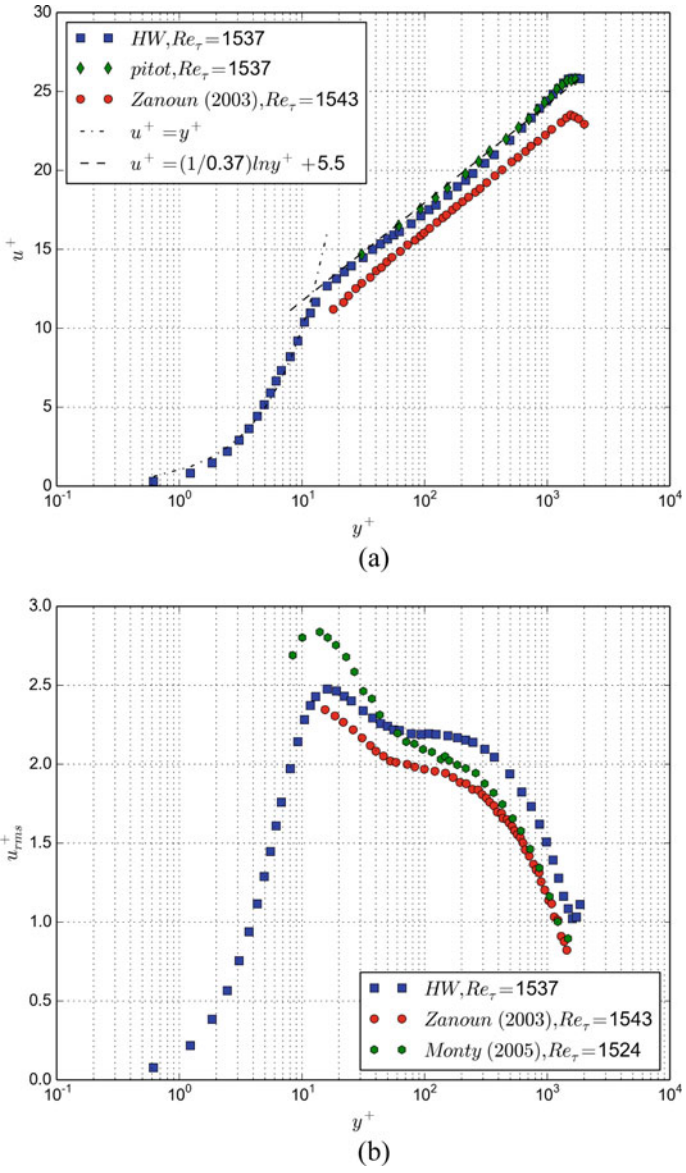

Fig. 2 Comparison of present HW data at $Re_\tau = 1537$ along with HW data of [7] at $Re_\tau = 1543$ for **a** mean velocity, **b** u_{rms}. The present mean velocity measured using Pitot at $Re_\tau = 1537$ is also included in **a**, HW data of [8] at $Re_\tau = 1524$ included in **b**

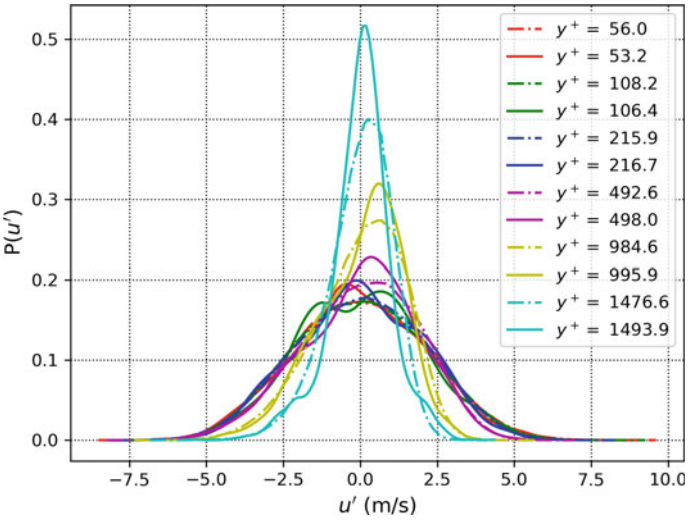

Fig. 3 PDF of fluctuating streamwise velocity for $Re_\tau = 1559$ using present PIV data (dashed lines) at various heights from the wall, plotted with PDF of fluctuating streamwise velocity from HW data for Re τ=1537 (solid lines) at similar wall-normal heights

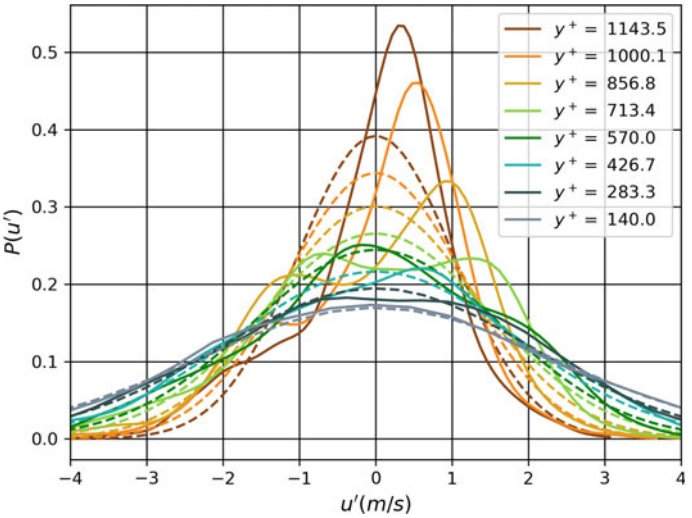

Fig. 4 PDF of fluctuating streamwise velocity for $Re_\tau = 1400$ at various heights from the wall plotted using PIV data (solid lines). The dashed lines denote the respective Gaussian curves with the same mean and standard deviation as the fluctuations at a given wall-normal location

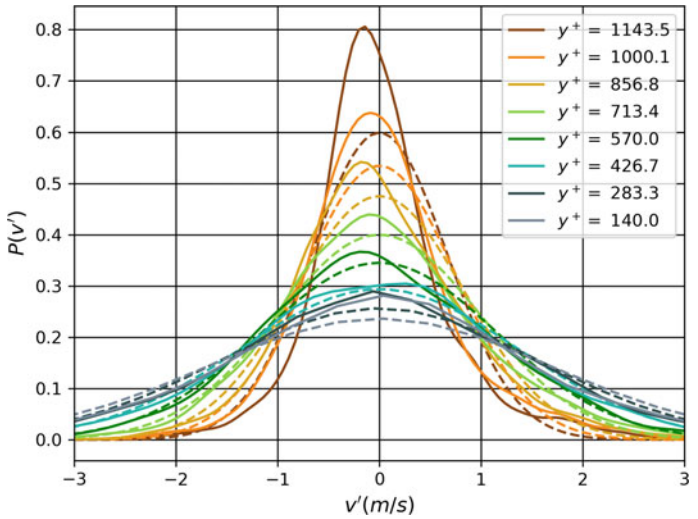

Fig. 5 PDF of fluctuating wall-normal velocity for $\mathrm{Re}_\tau = 1400$ at various heights from the wall plotted using PIV data (solid lines). The dashed lines denote the respective Gaussian curves with the same mean and standard deviation as the fluctuations at a given wall-normal location

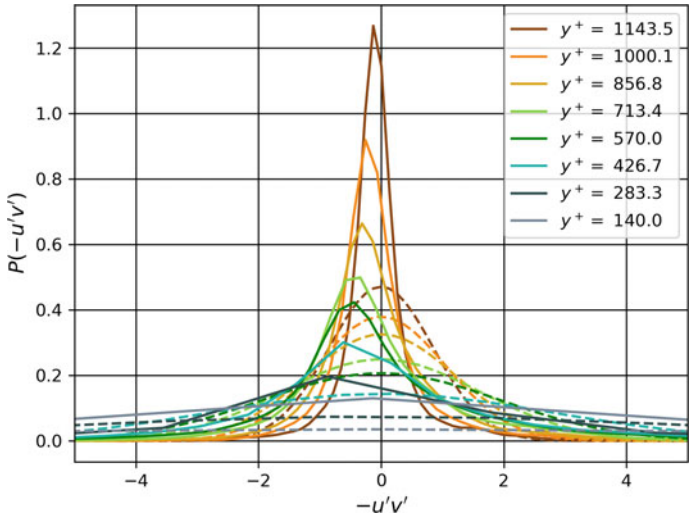

Fig. 6 PDF of fluctuating Reynolds stress for $\mathrm{Re}_\tau = 1400$ at various heights from the wall plotted using PIV data (solid lines). The dashed lines denote the respective Gaussian curves with the same mean and standard deviation as the fluctuations at a given wall-normal location

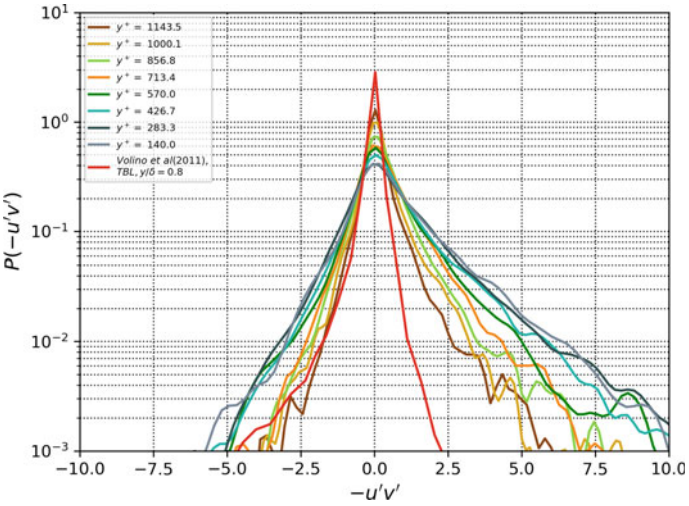

Fig. 7 PDF of fluctuating Reynolds stress for $Re_\tau = 1400$ at various heights from the wall plotted in loglog scale and compared with TBL data of [9] at $Re_\tau = 1772$, $y/\delta = 0.8$

The same PDF of $-u'v'$ is also plotted in semilog scale along with the result of [9] at a Reynolds number of $Re_\tau = 1772$ in Fig. 7. The peaky nature of the curve is more evident from this plot. The comparison with the data of [9] is fair. This also validates the use of PIV data to analyse PDFs.

4 Conclusions

The nature of PDFs of streamwise velocity, wall-normal velocity and Reynolds stress fluctuations is analysed for a turbulent channel flow using HW and PIV measurements. The HW measurements are validated with data from literature. The PDF calculated using the PIV data are in agreement with data from literature as well as with PDF calculated using present HW data. The PIV measurements capture the PDFs well albeit at a smaller acquisition sampling rate when compared to that of the HW. The PDFs of streamwise and wall-normal velocity fluctuations exhibit Gaussian behaviour close to the wall at least till the end of ISL, while the PDFs of Reynolds stress fluctuations exhibit non-Gaussian peaky behaviour throughout the channel, depicting the episodic description of bursting and turbulence production by ref. [3].

Acknowledgements The author wishes to profusely thank his research advisor, Prof. O. N. Ramesh of Indian Institute of Science Bangalore, India for the insightful and valuable discussions throughout the course of preparing this manuscript and the meticulous editing of the manuscript. The author expresses his sincere thanks to Defence Research and Development Organisation (DRDO), Ministry of Defence, Government of India and the Department of Science and Technology (DST), Ministry

of Science and Technology, Government of India for the PIV systems and the computers for data acquisition, which have been used extensively to obtain the data presented in this research article.

Nomenclature

CR	Contraction Ratio
d	Hotwire diameter [m]
HW	Hotwire
l	Hotwire active length [m]
κ	Karman constant
PDF	Probability Density Function
PIV	Particle Image Velocimetry
TBL	Turbulent Boundary Layer
TCF	Turbulent Channel Flow
Re_τ	Friction Reynolds number
u_τ	Friction Velocity [m/s]
U	Mean Streamwise Velocity [m/s]
u'	Fluctuating Streamwise Velocity [m/s]
v'	Fluctuating Wall-normal Velocity [m/s]
V	Voltage [V]
ν	Kinematic viscosity [m^2/s]
y	Wall-normal coordinate [m]
ZPG	Zero Pressure Gradient

References

1. Tsuji Y, Nakamura I (1999) Probability density function in the log-law region of low Reynolds number turbulent boundary layer. Phys Fluids 11(3):647–658
2. Lindgren B, Johansson AV, Tsuji Y (2004) Universality of probability density distributions in the overlap region in high Reynolds number turbulent boundary layers. Phys Fluids 16(7):2587–2591
3. Narasimha R, Kumar SR, Prabhu A, Kailas SV (2007) Turbulent flux events in a nearly neutral atmospheric boundary layer. Philos Trans Royal Soc A: Math, Phys Eng Sci 365(1852):841–858
4. Willmarth WW, Lu SS (1972) Structure of the Reynolds stress near the wall. J Fluid Mech 55(1):65–92
5. Raghuram S, Ramesh ON (2021) Delayed transition in a plane channel flow with high contraction ratio. Exp Fluids 62(7):1–9
6. Durst F, Zanoun E-S, Pashtrapanska M (2001) In situ calibration of hot wires close to highly heat-conducting walls. Exp Fluids 31(1):103–110
7. Zanoun E-S (2003) Answers to some open questions in wall-bounded laminar and turbulent shear flows, Ph.D. thesis
8. Monty JP (2005) Developments in smooth wall turbulent duct flows, Ph.D. thesis, p 272
9. Volino RJ, Schultz MP, Flack KA (2011) Turbulence structure in boundary layers over periodic two-and three-dimensional roughness. J Fluid Mech 676:172–190